Petroleum Science 20 (2023) 3400–3410

Contents lists available at ScienceDirect

Petroleum Science

journal homepage: www.keaipublishing.com/en/journals/petroleum-science

Original Paper

Petrophysical parameters inversion for heavy oil reservoir based on a laboratory-calibrated frequency-variant rock-physics model

Xu Han [a], Shang-Xu Wang [a, b], Zheng-Yu-Cheng Zhang [a], Hao-Jie Liu [c], Guo-Hua Wei [c], Gen-Yang Tang [a, b, *]

[a] CNPC Key Laboratory of Geophysical Prospecting, China University of Petroleum (Beijing), Beijing, 102249, China
[b] Engineering Research Center of the Ministry of Education for Exploration and Development of Complex Oil and Gas Reservoirs, China University of Petroleum (Beijing), Beijing, 102249, China
[c] Shengli Oilfield Geophysical Exploration Research Institute, Sinopec, Dongying, 257000, Shandong, China

ARTICLE INFO

Article history:
Received 5 August 2022
Received in revised form
13 May 2023
Accepted 30 June 2023
Available online 3 July 2023

Edited by Jie Hao and Meng-Jiao Zhou

Keywords:
Heavy oil
Rock physics
Velocity dispersion
Pre-stack inversion
Reservoir prediction

ABSTRACT

Heavy oil has high density and viscosity, and exhibits viscoelasticity. Gassmann's theory is not suitable for materials saturated with viscoelastic fluids. Directly applying such model leads to unreliable results for seismic inversion of heavy oil reservoir. To describe the viscoelastic behavior of heavy oil, we modeled the elastic properties of heavy oil with varying viscosity and frequency using the Cole-Cole-Maxwell (CCM) model. Then, we used a COherent Potential Approximation (CPA) instead of the Gassmann equations to account for the fluid effect, by extending the single-phase fluid condition to two-phase fluid (heavy oil and water) condition, so that partial saturation of heavy oil can be considered. This rock physics model establishes the relationship between the elastic modulus of reservoir rock and viscosity, frequency and saturation. The viscosity of the heavy oil and the elastic moduli and porosity of typical reservoir rock samples were measured in laboratory, which were used for calibration of the rock physics model. The well-calibrated frequency-variant CPA model was applied to the prediction of the P- and S-wave velocities in the seismic frequency range (1–100 Hz) and the inversion of petrophysical parameters for a heavy oil reservoir. The pre-stack inversion results of elastic parameters are improved compared with those results using the CPA model in the sonic logging frequency (~10 kHz), or conventional rock physics model such as the Xu-Payne model. In addition, the inversion of the porosity of the reservoir was conducted with the simulated annealing method, and the result fits reasonably well with the logging curve and depicts the location of the heavy oil reservoir on the time slice. The application of the laboratory-calibrated CPA model provides better results with the velocity dispersion correction, suggesting the important role of accurate frequency dependent rock physics models in the seismic prediction of heavy oil reservoirs.

1. Introduction

The increasing demand for hydrocarbon energy has renewed interest in the exploitation of bitumen and heavy oil reservoirs. The world's heavy oil reserves exceed 6 trillion barrels, three times the world's conventional oil and natural gas reserves (Batzle et al., 2006). However, unlike light oils, heavy oils have high density and viscosity, and exhibit viscoelastic properties (Behura et al., 2007). Simple empirical trends in fluid properties (such as viscosity, density, gas-oil ratio) developed for light oils are not applicable to heavy oils (Han et al., 2007b). Compared with conventional reservoir rocks, the petrophysical properties of heavy oil saturated rocks are not well understood. Many classic rock physics theories such as Gassmann equation are not applicable to heavy oil reservoirs, which poses great challenges to the reservoir prediction of heavy oil reservoirs (Yuan et al., 2019).

In addition, the semi-solid behavior of heavy oil causes the material to have an effective shear modulus and the ability to propagate shear waves. The velocity and modulus of heavy oil have a strong dependence on viscosity and frequency. Experimental

* Corresponding author.
E-mail address: tanggenyang@163.com (G.-Y. Tang).

https://doi.org/10.1016/j.petsci.2023.06.011

results for rocks saturated with heavy oil in the seismic frequency band (10–100 Hz), ultrasonic band (10^5–10^6 Hz) and sonic logging (10^4 Hz) measurements may be completely different (Batzle et al., 2006). Previous experimental studies have shown that heavy oil is a kind of fluid with viscoelastic properties, and its modulus has strong dependence on frequency and viscosity (Nur et al., 1984; Eastwood, 1993; Schmitt, 1999; Batzle et al., 2006; Behura et al., 2007; Han et al., 2007a). The elastic modulus of heavy oil saturated rock decreases sharply with the decrease of viscosity, and the main factor causing the decrease of velocity is the change of fluid properties with viscosity (Behura et al., 2007; Tosaya et al., 1987; Batzle et al., 2006). Han et al. (2007a, 2007b, 2008) measured the relationship between the velocities of heavy oil saturated rock under ultrasonic frequency band with temperature, and found that the velocity of saturated heavy oil sandstone decreased significantly with the increase of temperature. Recently, Yuan et al. (2016, 2017) measured the velocity of heavy oil sandstone under different pressure and temperature conditions using hot steam and quantitatively characterized the pressure and temperature dependence of the velocity of heavy oil sandstone. Yuan et al. (2019) measured heavy oil sand under different physical conditions and calculated the attenuation of heavy oil sand under different pressure and temperature conditions using the spectral ratio method. Due to the viscoelastic characteristics of heavy oil, the existing pore medium theories are no longer suitable for establishing the rock physics model of heavy oil reservoirs. Many researchers have done a lot of research on petrophysical modeling of heavy oil reservoirs (Ciz and Shapiro, 2007; Han et al., 2007a; Gurevich et al., 2008; Das and Batzle, 2008; Russell et al., 2011; Yuan and Han., 2013). Ciz and Shapiro (2007) proposed that the generalized Gassmann equation can be used for fluid replacement in heavy oil reservoirs to calculate the elastic modulus of rocks saturated with heavy oil. Gurevich et al. (2008) proposed to use the coherent potential approximation method to estimate the elastic parameters of heavy oil-bearing rocks, and gave the variation characteristics of rock velocity with frequency. Makarynska et al. (2010) used the CPA model as a fluid substitution method for viscous fluids. Yuan et al. (2016) developed a rock physics model for saturated fluid heavy oil sands, using heavy oil as part of the rock frame to describe the temperature dependence of the elastic parameters of the sandstone frame. Zhao et al. (2017) considered fluid fluidity into the heavy oil model and demonstrated that changes in fluidity lead to changes in seismic frequencies.

Considering the influence of frequency dispersion, the joint inversion of seismic data with logging data will cause systematic errors, especially for heavy oil reservoirs, which are saturated viscoelastic fluids. Therefore, it is necessary to establish a frequency dependent rock-physics model suitable for heavy oil reservoirs to avoid this error, and calibrate the rock physics model using laboratory measurement results. This model can provide guidance and help for seismic inversion and prediction of heavy oil reservoirs. The S-wave velocity logging curve plays an important role in the inversion of seismic data and the calculation of rock physical parameters of the formation. However, only a few of the development wells have S-wave velocity curve. In the absence of S-wave velocity curve, it is more important to predict S-wave logging data from P-wave logging data or other logging curve. In addition, S-wave velocity curve is also required in pre-stack seismic inversion. The inversion of pre-stack seismic data requires a constraint on the logging velocity. However, for viscoelastic fluids like heavy oil, heavy oil reservoirs have significant frequency dependence. If the logging data is applied directly to the seismic data inversion may bring some errors. Therefore, the logging velocity is needed to be calibrated to the seismic frequency band (30 Hz) to obtain more reliable pre-stack inversion results.

In this study, we established a frequency-variant rock physics model suitable for a heavy oil reservoir in eastern China. Based on the rock physics model, we performed pre-stack inversion and reservoir prediction in the working area. First, we measured physical and elastic parameters of heavy oil and samples. Then, we use the Cole-Cole-Maxwell (CCM) model and Coherent Potential Approximation (CPA) model as the fluid substitution method of viscoelastic fluid saturated rock, extending the single-phase fluid condition to the two-phase fluid condition (heavy oil and water) so that partial saturation of the heavy oil can be considered. Based on experimental measurements (heavy oil and samples), we calibrated the CCM model and the CPA model. We used a modified CPA model to predict logging velocity in heavy oil reservoirs. The input parameters required by the model are provided by logging data. The CPA model can correct the logging velocity to seismic frequency band (30 Hz). Finally, based on the calculated results of the frequency-corrected logging velocity (30 Hz), we performed seismic pre-stack inversion for the working area, and invert the porosity of heavy oil reservoir using simulated annealing method.

2. Rock physics model

2.1. CCM model

Heavy oil exhibits Newtonian fluid properties at low frequencies, and the properties are similar to elastic solids at high frequencies. Between these two extremes, the propagation of waves in heavy oil is dispersive and exhibits strong attenuation (Batzle et al., 2006). When the rock is filled with heavy oil, the rock will also exhibit viscoelastic properties. Therefore, in order to study the elastic properties of rock saturated with heavy oil, we first need to study the viscoelastic properties of heavy oil. And the frequency dependence of the shear modulus of heavy oil can be calculated by the Cole-Cole model (Cole and Cole, 1941; Gurevich et al., 2008), which combines the shear modulus with the high and low frequency limits. The shear modulus and the angular frequency under the relaxation time are related:

$$\mu_f = \mu_0 + \frac{\mu_\infty - \mu_0}{\frac{1}{(-i\omega\tau)^\beta} + 1} \tag{1}$$

where, μ_∞ and μ_0 is the shear modulus of the heavy oil under the limit conditions of high and low frequency, $\beta < 1$ is an adjustable parameter. $\tau = \eta/\mu_\infty$ is the relaxation time, η is dynamic shear viscosity. The relaxation time depends on the viscosity of the fluid and is a function of temperature. However, the complex shear modulus of the Cole-Cole model tends to be μ_0 under the extreme low-frequency conditions. This is contrary to our understanding of oil (oil behaves as a Newtonian fluid under low-frequency extreme conditions). Gurevich et al. (2008) synthesized the Cole-Cole model and the Maxwell model, and established a CCM model.

$$\mu_f = \frac{\mu_\infty}{\frac{1}{(-i\omega\tau)} + \frac{1}{(-i\omega\tau_1)^\beta} + 1} \tag{2}$$

where $\tau = \eta/\mu_\infty$ and τ_1 are two points of the relaxation spectrum. When $\tau/\tau_1 \gg 1$, the CCM model is close to the Cole-Cole model; whereas, for $\tau/\tau_1 \to 0$, the CCM model is close to the Maxwell model.

We measured the viscosity of the heavy oil samples from the working area with a Brookfield viscometer (LVT230) and the shear modulus of the heavy oil with a viscosity of $\mathrm{Log}_{10}\eta = 8.3$Pa•s under different frequencies with a torsion probe. The fitting parameters (pore aspect ratio) of the CCM model were adjusted using the

experimental measurement results to obtain a CCM model suitable for heavy oil. Fig. 1 shows the results of the variation of viscosity and density of heavy oil with temperature, which decreases with the increase of temperature. Fig. 2 shows the relationship between the shear modulus of heavy oil calculated by the CCM model under different viscosity and the frequency. The shear modulus of heavy oil is strongly dependent on frequency and viscosity. Under high viscosity conditions, heavy oils have high shear modulus and exhibit solid properties. With the viscosity decreases, the shear modulus gradually increases with frequency, with a transition zone from Newtonian fluid to non-Newtonian fluid. With the decrease of viscosity, the transition zone of the shear modulus gradually shifts to high frequency. When the viscosity is lower than 1.44 Pa s, the shear modulus can no longer be observed.

2.2. CPA model

We mainly use the Coherent Potential Approximation method (CPA) proposed by Makarynska et al. (2010) as a fluid substitution method for saturated viscous fluid rocks. One of the main properties of CPA is that it has symmetry with respect to each component. In this method, each component is treated equally, that is, no component is the main component, and a large number of components are used as the load-bearing component (Makarynska et al., 2010). CPA model is solved by iteration:

$$K_{n+1} = \frac{\varphi K_f P_n^f + (1-\varphi) K_s P_n^s}{\varphi P_n^f + (1-\varphi) P_n^s} \tag{3}$$

$$G_{n+1} = \frac{\varphi G_f Q_n^f + (1-\varphi) G_s Q_n^s}{\varphi Q_n^f + (1-\varphi) Q_n^s} \tag{4}$$

where, K_f and G_f are the bulk and shear modulus of the pore filler (heavy oil in our case); K_s and G_s are the bulk modulus and shear modulus of the rock matrix; φ is the porosity; P and Q are the invariants of the Wu tensor (Wu, 1966). The expressions of P and Q can be found in Berryman (1980). α is the pore aspect ratio. The components of this tensor depend on the aspect ratio of the pore, the bulk modulus and shear modulus of the pore filler, the effective modulus K and G of the matrix material and the composite material. The iterative process needs to first use the Voigt-Reuss-Hill average to calculate K_1 and G_1. This scheme was used to calculate the elastic modulus of rock dry skeleton by setting the bulk modulus and shear modulus of the saturated fluid to zero (Makarynska et al., 2010).

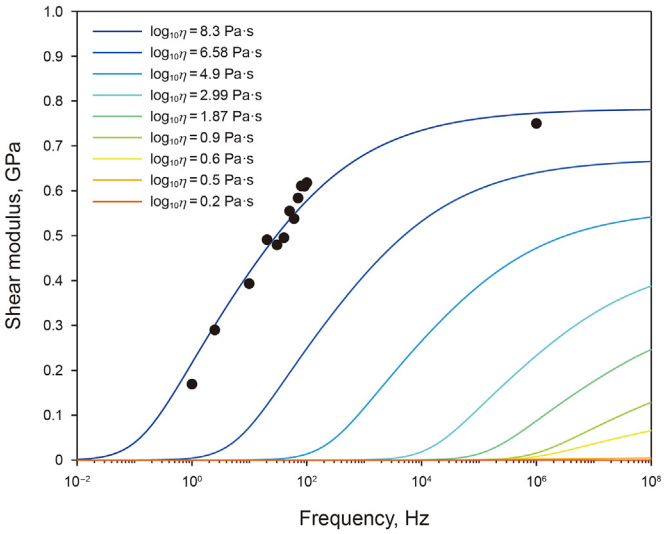

Fig. 2. The relationship between the complex shear modulus of heavy oil calculated by the CCM model under different viscosity and frequency; the points represent the measured results of the shear modulus of heavy oil.

We collected a large number of cores from the heavy oil reservoir in eastern China and measured the porosity and velocities of these samples. These samples have a wide range of porosity (1%–30%) and the lithology is shaly sandstone. We calculated elastic moduli for different porosity and pore aspect ratios under dry conditions using the CPA model. The simulation results show in Fig. 3 and compared with the ultrasonic experimental measurement results. Model parameters: $K_s = 34$ GPa, $G_s = 28$ GPa, $K_f = 0$ GPa, $G_f = 0$ GPa. When the pore shape changes from low-to high-aspect ratio, the elastic modulus changes from a nonlinear to linear trend with porosity. It is found that the experimental measurement results are generally distributed around the curve with the pore aspect ratio of 0.1. Therefore, the CPA model with a pore aspect ratio of 0.1 is more suitable for the working area. Due to the viscoelastic properties of heavy oil, the rock saturated with heavy

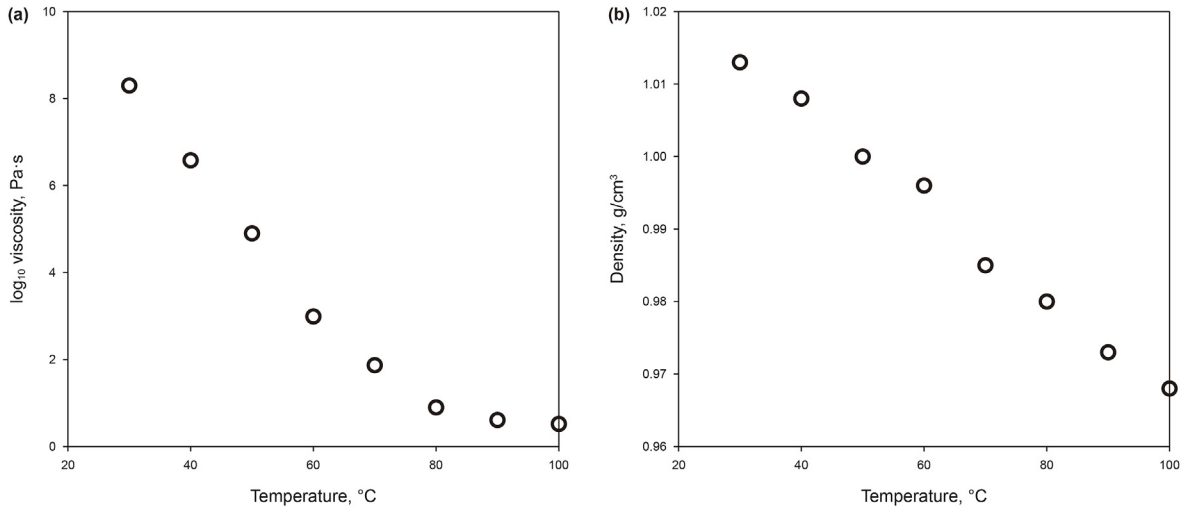

Fig. 1. The results of viscosity and density of heavy oil with temperature.

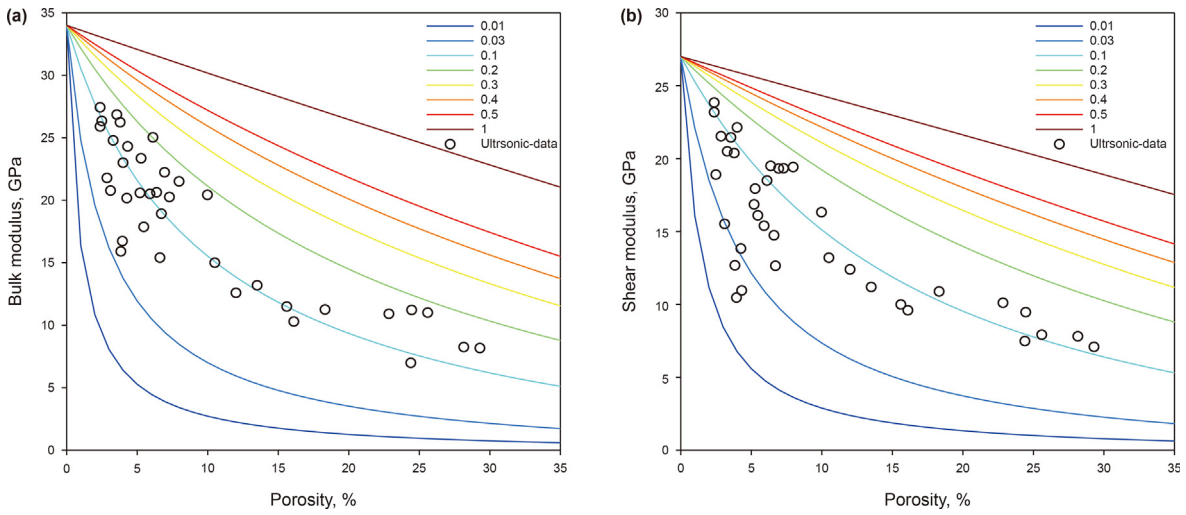

Fig. 3. The relationship between elastic parameters and porosity of the sandstone under different pore aspect ratios superimposed with actual measurement results of the reservoir sandstone samples from the working area.
(a) Bulk modulus; (b) Shear modulus.

oil also has viscoelasticity. Here we combine the CCM model and the CPA model to calculate the relationship between elastic modulus and frequency under different viscosity conditions. As shown in Fig. 4, the saturated heavy oil rock has obvious dispersion phenomenon. With the decrease of viscosity, the dispersion range of elastic modulus gradually moves to high frequency. When the viscosity is lower than 1.44 Pa s, there is no obvious dispersion phenomenon.

The pore fluids in the heavy oil reservoirs include heavy oil, brine and/or gas. We modified the CPA model so that the pore phase can contain two fluids, brine and heavy oil, and both heavy oil and brine are used as pore inclusions. Therefore, through the CPA model, we can divide the pore phase into two parts: brine and heavy oil. The elastic parameters of the rock saturated with two fluids are calculated with

$$K_{n+1}=\frac{S_o\varphi K_{oil}P_n^{oil}+(1-S_o)\varphi K_{water}P_n^{water}+(1-\varphi)K_sP_n^s}{S_o\varphi P_n^{oil}+(1-S_o)\varphi P_n^{water}+(1-\varphi)P_n^s} \quad (5)$$

$$G_{n+1}=\frac{S_o\varphi G_{oil}Q_n^{oil}+(1-S_o)\varphi G_{water}Q_n^{water}+(1-\varphi)G_sQ_n^s}{S_o\varphi Q_n^{oil}+(1-S_o)\varphi Q_n^{water}+(1-\varphi)Q_n^s} \quad (6)$$

where, K_{oil} and G_{oil} are the bulk modulus and shear modulus of heavy oil, K_{water} and G_{water} are the bulk modulus and shear modulus of brine, and S_o is the oil saturation.

Fig. 5 shows the results of bulk and shear modulus of rock saturated with heavy oil and brine as a function of frequency and saturation. The viscosity of the heavy oil is $\mathrm{Log}_{10}\eta = 6.58$Pa·s. When the rock is completely saturated with water, the bulk and shear modulus of simulation result have no dispersion phenomenon. With the increase of oil saturation, the bulk and shear modulus gradually increase, and the absolute dispersion gradually increases.

3. Application of rock physics model

3.1. S-wave prediction

The S-wave velocity logging curve plays an important role in the

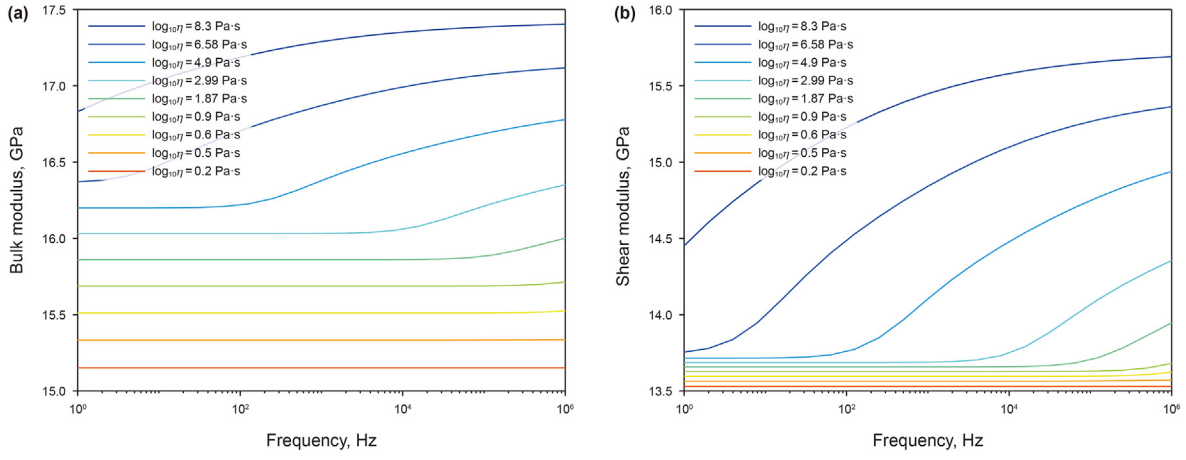

Fig. 4. The relationship between elastic parameters and frequency simulated by the modified CPA model under different viscosity.
(a) Bulk modulus; (b) Shear modulus.

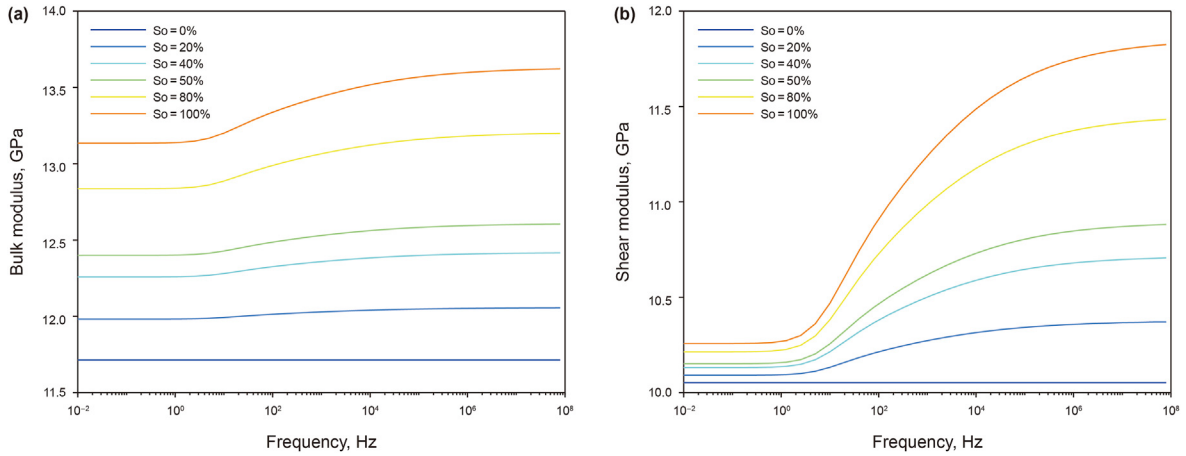

Fig. 5. The relationship between elastic parameters and frequency under different oil saturation conditions simulated by the modified CPA model. (a) Bulk modulus; (b) Shear modulus.

inversion of seismic data and the calculation of rock physical parameters of the formation. However, only a few of the development wells have S-wave velocity curve. In the absence of S-wave velocity curve, it is more important to predict S-wave logging data from P-wave logging data or other logging curve. In addition, S-wave velocity curve is also required in pre-stack seismic inversion. Fig. 6 shows the working flow chart of this study.

We used the modified CPA model and the Xu-Payne model (Xu and Payne, 2009; Makarynska et al., 2010) to calculate the S-wave curve of heavy oil reservoirs. The physical parameters (saturation, shale content, porosity) required by the rock physical model are all derived from logging data, and the elastic parameters of heavy oil are obtained through the CCM model. In the process of simulating logging S-wave velocity, we proposed a constraint parameter: pore aspect ratio. By adjusting this parameter, the error between the P-wave velocity calculated by the actual logging P-wave velocity and the model is minimized, and finally the S-wave velocity is estimated. We performed the S-wave curve calculation in the working area. Taking Well H as an example, Fig. 7 shows the logging data and S-wave curve prediction results. The heavy oil reservoir section of Well H is 2510–2600 m, the lower layer is a tight sandstone layer and the upper layer is a clay layer. By adjusting the constraint parameters, the P-wave velocity curve calculated by the model has a high fitting degree with the logging P-wave curve. The pore aspect ratio of the heavy oil reservoir section is about 0.1, matching those estimated from laboratory measurements. For Well H, the velocity prediction results of the Xu-Payne model are much similar as the results of the modified CPA model at the sonic logging frequency.

Due to the viscoelastic properties of rocks saturated with heavy oil, the elastic parameters of the samples have obvious frequency dependence. Before inversion, we corrected the log data to the seismic frequency band (30 Hz) using the modified CPA model to

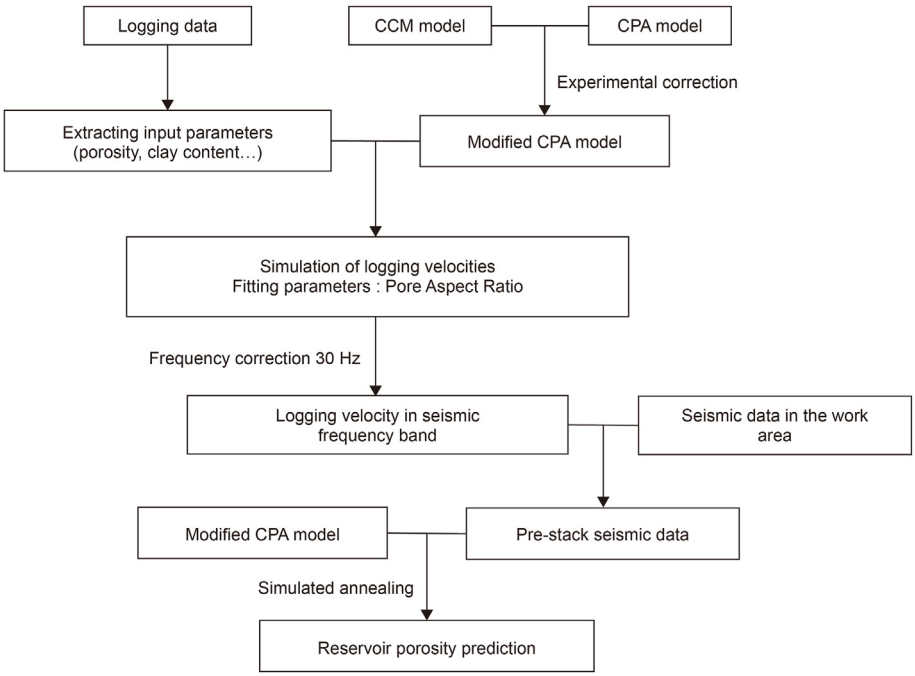

Fig. 6. The working flow chart of this study.

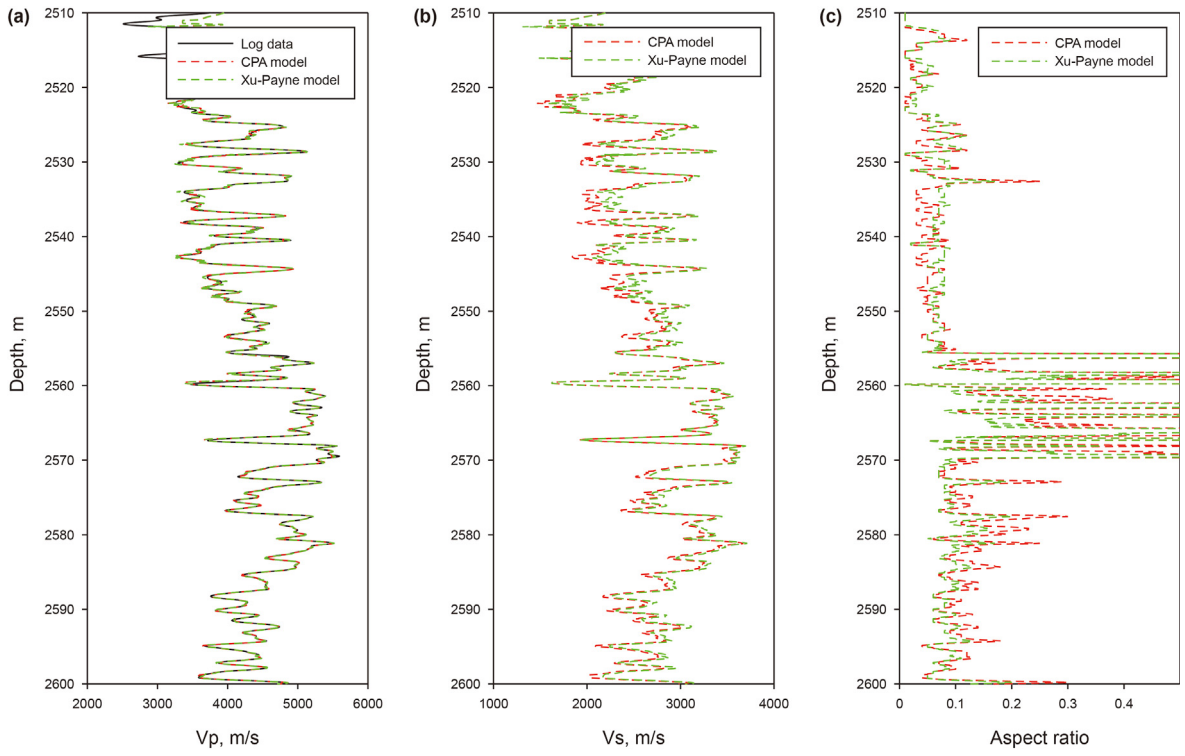

Fig. 7. Well H logging data and prediction results of CPA model and Xu-Payne model. (a) P-wave velocity curve; (b) S-wave velocity curve; (c) Pore aspect ratio curve.

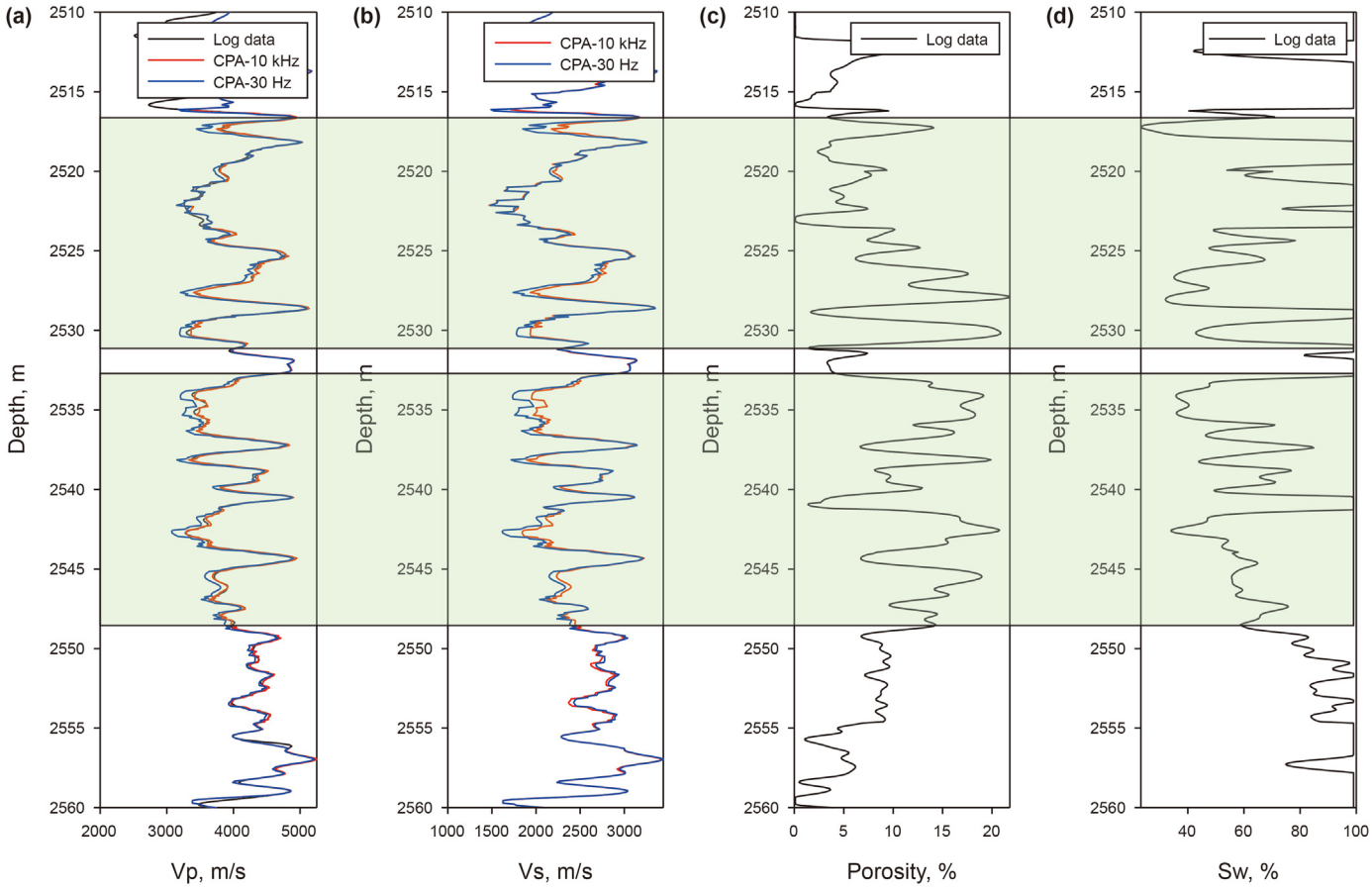

Fig. 8. Well H logging velocity at different frequencies calculated by the modified CPA model.

calculate both Vs and Vp. We took the pore aspect ratio curve obtained from the inversion as an input parameter. By modifying the frequency, we calculated the logging velocity in the seismic frequency band (30 Hz). Fig. 8 is the log velocity at different frequencies calculated by the modified CPA model. In the high water saturation range, the velocities in the seismic frequency band are basically equal to the velocities at the logging frequency. In the high oil saturation range, the velocity in the seismic frequency range is smaller than that in the logging frequency band. Therefore, for heavy oil reservoirs, it is necessary to perform frequency correction on logging data to obtain more reasonable seismic inversion results.

The pre-stack inversion of seismic data requires the constraint of logging S-wave velocity, but most logging data does not contain S-wave velocity information. The Vs of the heavy oil reservoir section of all wells in the block is predicted by the modified CPA model, and the logging velocities were calibrated to the seismic frequency band (30 Hz). The non-reservoir formation has a higher clay content. We used the empirical formula of "mudrock line" to calculate the S wave velocity for these formations.

3.2. Pre-stack seismic inversion

We performed the pre-stack seismic inversion for the whole working area with the P- and S-wave velocity models which were calibrated to 30 Hz. We also analyzed the logging data from well H, and the results are shown in Fig. 9. We can use Vp/Vs to distinguish mudstone (1.7–2.3) and sandstone (1.5–1.7). Tight sandstone (11000-15000 m/s·g/cc) and heavy oil reservoirs (9000–11000 m/s·g/cc) can be distinguished using P-wave impedance. In addition, the impedance range of mudstone is 6000–10000 m/s·g/cc. Therefore, we can identify heavy oil reservoirs by combining the results of Zp and Vp/Vs.

We took the profile of Well H extracted from the inversion results as an example for analysis. The time range of the inversion result is from horizon T4 to 50ms below horizon T6. The Zp and Vp/Vs results of the pre-stack inversion based on the Vs calculated by the modified CPA model and Xu-Payne model are shown in Fig. 10. Among them, the Vs predicted by the modified CPA model has two frequency bands (30 Hz and 1 kHz). Based on the log data analysis results, we can determine that the heavy oil reservoirs are characterized by low Zp and Vp/Vs. Tight sandstones are characterized by high Zp and low Vp/Vs. Mudstone is characterized by high Vp/Vs and low Zp. The heavy oil reservoirs are roughly distributed from layer T6 to 10ms above layer T6, and the corresponding depth range is 2510 m–2560 m. Tight sandstones are distributed in the range from layer T6 to 10 ms below layer T6, and the corresponding depth ranges from 2560 m to 2600 m, which is the base of heavy oil reservoirs. Mudstone is distributed within 10 ms on the layer T6, and the corresponding depth range is more than 2510 m, which is the overlying layer of the heavy oil reservoir. Fig. 10a, 10c, 10e are the pre-stack inversion results of Zp profiles. Near Well H, we can distinguish the tight sandstone under the T6 layer from the heavy oil reservoir and mudstone above the T6 layer. The P-wave impedance of the heavy oil reservoir ranges from 9000 to 10500 m/s·g/cc, which is shown in red. The P-wave impedance of tight sandstones ranges from 10500-14000 m/s·g/cc and appears blue. The P-wave impedance of mudstone ranges from 8500 to 9500 m/s·g/cc and appears red-yellow. Fig. 10b, 10d,10f are the inversion results of Vp/Vs profiles. Near Well H, we can clearly distinguish between sandstone layers and mudstone layers. The Vp/Vs of the heavy oil reservoir ranges from 1.65 to 1.75, which is shown in cyan. The Vp/Vs range of tight sandstone is 1.4–1.65 and appear blue. The Vp/Vs range of mudstone is 1.75–2 and appears red. Fig. 10c, 10d are pre-stack inversion profiles of Zp and Vp/Vs based on logging data predicted by CPA model in the seismic frequency band. Compared with the inversion results based on logging data at 10 kHz, the Zp profile can better distinguish between heavy oil reservoirs and mudstones. The Vp/Vs profile can better distinguish heavy oil reservoirs and tight sandstones. Therefore, by comprehensively analyzing Zp and Vp/Vs profiles, the inversion results based on frequency-corrected logging data can better distinguish heavy oil reservoirs, tight sandstones and mudstones.

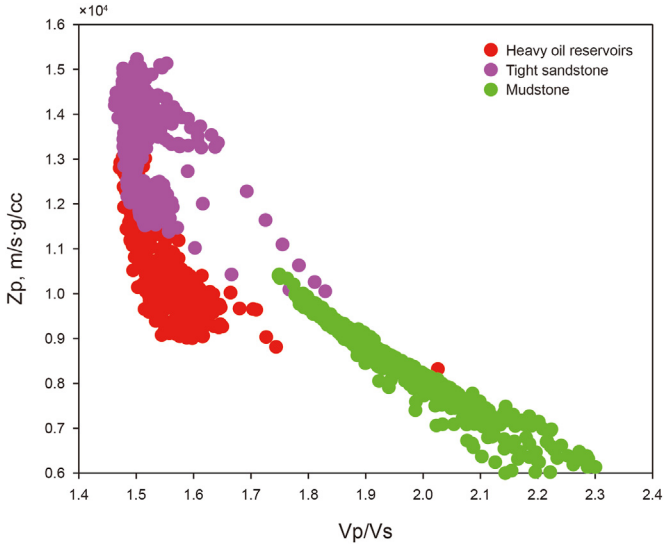

Fig. 9. Intersection map of P-wave impedance and Vp/Vs.

The heavy oil reservoirs are mainly distributed in the range from layer T6 to 10 ms above layer T6. In order to study the distribution of heavy oil reservoirs, we make horizontal slices at 10 ms above layer T6 and 10 ms below layer T6. Fig. 11 is the slice result of Zp and Vp/Vs pre-stack inversion base on logging data predicted by modified CPA model in seismic frequency band (30 Hz). Fig. 11a, 11b are the slice result of Zp and Vp/Vs at 10 ms above layer T6. The heavy oil reservoirs appear red in the Zp results, and blue in the Vp/Vs results. It can be found from the Zp and Vp/Vs slice results that the favorable heavy oil reservoirs are mainly distributed in the areas near well-H and well-E. Fig. 11c, 11d are the slice result of Zp and Vp/Vs at 10ms below layer T6. P-wave impedances near well-H and well-E are shown in blue, and Vp/Vs in purple. This area is tight sandstone, the basement of heavy oil reservoirs. This result is consistent with the well crossing section (the tight sandstone basement is below the layer T6). Fig. 12 is the slice result of Zp and Vp/Vs pre-stack inversion based on logging data predicted by Xu-Payne model. Compared with the inversion results with the Xu-Payne model, the modified CPA model is more suitable for heavy oil reservoirs. The logging data predicted by the modified CPA model can be more reasonably applied to pre-stack seismic inversion.

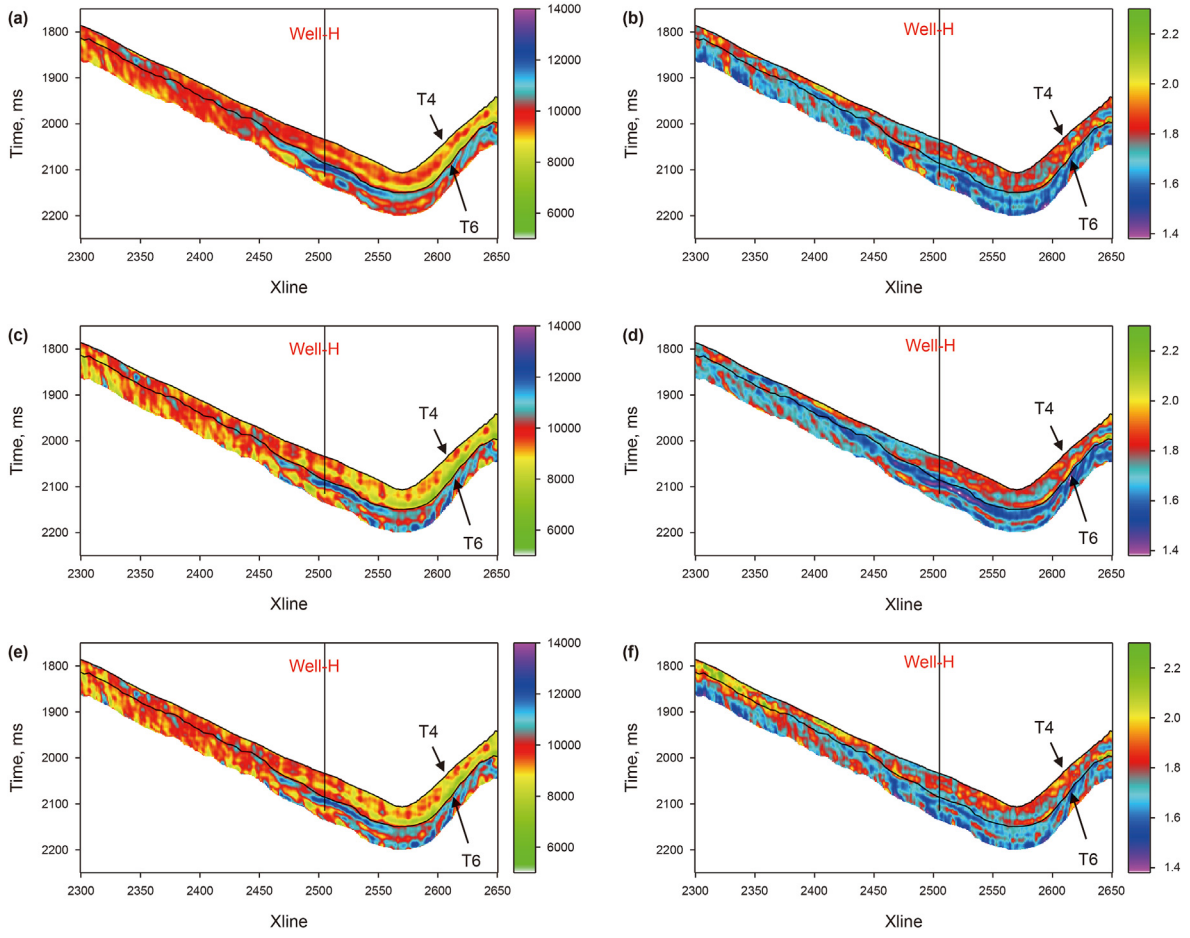

Fig. 10. Pre-stack inversion results of cross well profile (take inline2339 as an example). (a, b) Zp and Vp/Vs pre-stack inversion profiles based on CPA model (10 kHz); (c, d) Zp and Vp/Vs pre-stack inversion profiles based on CPA model (30 Hz); (e, f) Zp and Vp/Vs pre-stack inversion profiles based on Xu-Payne model (10 kHz).

Based on the modified CPA model and the pre-stack inversion results, we used the simulated annealing method to invert the reservoir petrophysical parameters (porosity). The petrophysical parameters are mainly divided into elastic (velocity, modulus) and physical (density, porosity et al.) parameters. In this paper, we mainly invert the porosity of heavy oil reservoirs. The inversion results are adjusted by controlling parameters until the objective function reaches a global minimum. We invert the porosity of heavy oil reservoirs by taking the minimum value between the pre-stack inversion results and the simulation results of the modified CPA model. Taking the profile of Well-H (inline 2339) as an example, the prediction result of the porosity profile is shown in Fig. 13a. The porosity of heavy oil reservoirs ranges from 8% to 14%. The porosity of the mudstone above the heavy oil reservoir is 5%–8%, and the porosity of the tight sandstone below the heavy oil reservoir is less than 5%. The prediction results of the porosity of heavy oil reservoirs are relatively accurate. We compared the inversion results of the porosity of Well-H with the log porosity, the results show in Fig. 13b. This fitting results between the porosity calculated by the simulated annealing method and the logging porosity are good, indicating that the method can accurately predict the porosity of heavy oil reservoirs. We made porosity predictions for the horizontal slices at 10ms above layer T6, and the results are shown in Fig. 14. The favorable heavy oil reservoirs near Well-H and well-E have porosity ranging from 8% to 11%. This range is a heavy oil reservoir, which is consistent with the pre-stack inversion results. This demonstrates the applicability of the method.

4. Conclusions

The elastic modulus of rocks saturated with heavy oil are viscosity- and frequency-dependent. We used the CPA model as a fluid replacement method for heavy oil saturated rock and the CCM model to characterize the viscoelastic properties of heavy oil. The results suggest that the combination of CCM and CPA model can well describe the viscoelastic properties of rocks saturated with heavy oil. We modified the CPA model so that it can describe the elastic properties of rocks with two-phase fluids (heavy oil and brine) in the pore space. The modified CPA model established the relationship between the elastic parameters of saturated heavy oil rock with viscosity, frequency and saturation, and calibrated the rock physics model with experimental data. We applied the modified CPA model to an actual heavy oil field, use a well-calibrated frequency-dependent CPA model to predict log velocities in the seismic frequency range (~30 Hz), and perform a combined log-seismic pre-stack inversion. These results show that the inversion results of elastic parameters are much improved compared with those results using the CPA model or traditional petrophysical models such as the Xu-Payne model in the sonic logging frequency (about 10 kHz). In addition, the inversion of the porosity of the reservoir was conducted with the simulated annealing method, and the result fits reasonably well with the logging curve and depicts the location of the heavy oil reservoir on

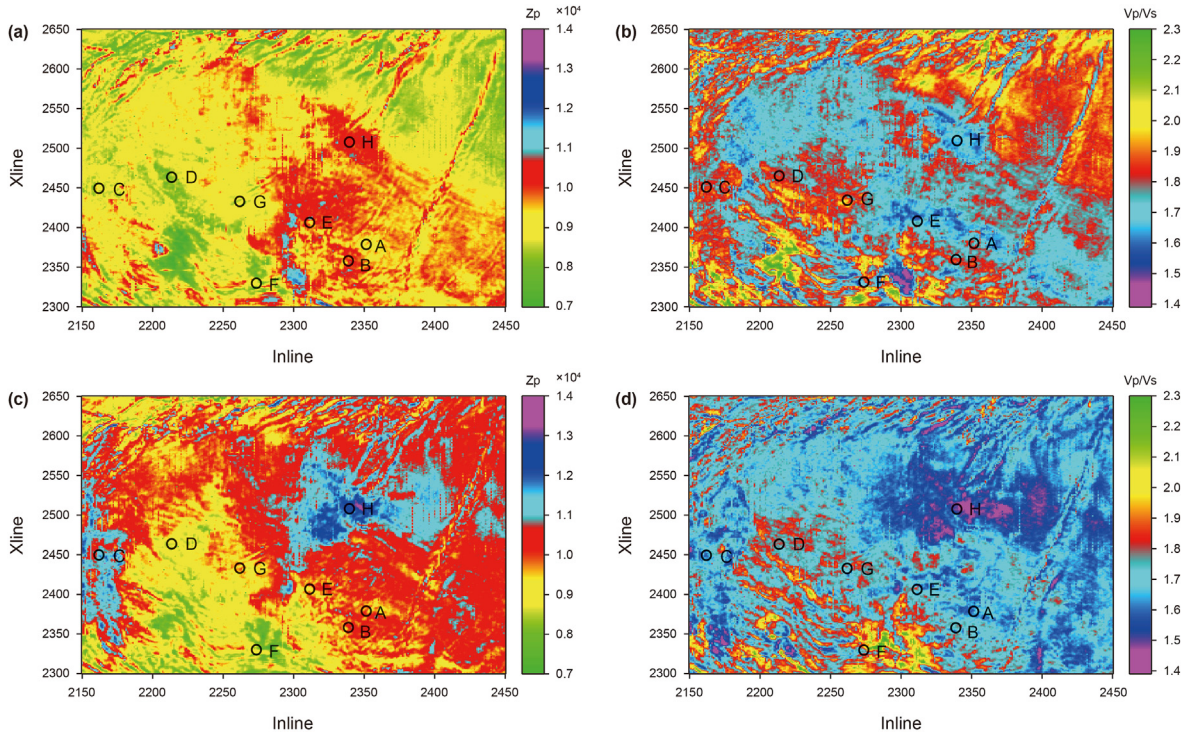

Fig. 11. The slice result of Zp and Vp/Vs pre-stack inversion base on logging data predicted based on the modified CPA model in seismic frequency band (30 Hz). (a) Zp slice at 10 ms above layer T6; (b) Vp/Vs slice at 10 ms above layer T6; (c) Zp slice at 10 ms below layer T6; (d) Vp/Vs slice at 10 ms below layer T6. The heavy oil reservoirs appear red in the Zp results, and blue in the Vp/Vs results.

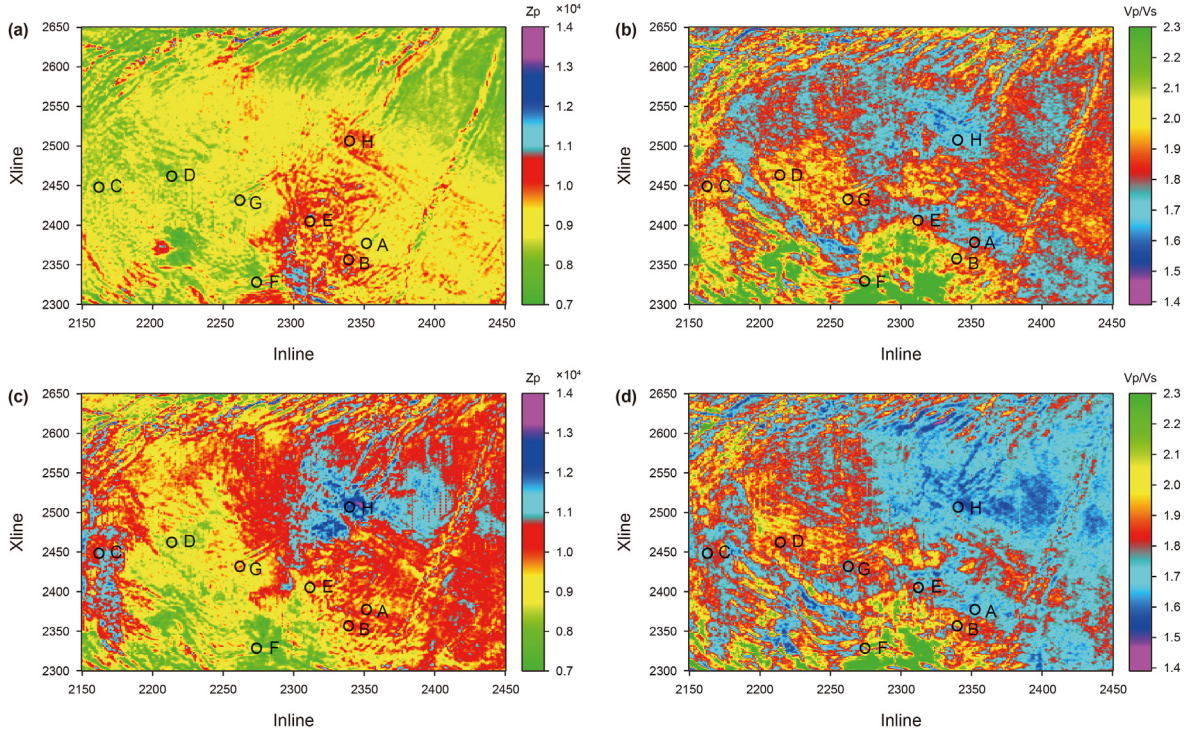

Fig. 12. The slice result of Zp and Vp/Vs pre-stack inversion base on logging data predicted based on Xu-Payne model. (a) Zp slice at 10 ms above layer T6; (b) Vp/Vs slice at 10 ms above layer T6; (c) Zp slice at 10 ms below layer T6; (d) Vp/Vs slice at 10 ms below layer T6.

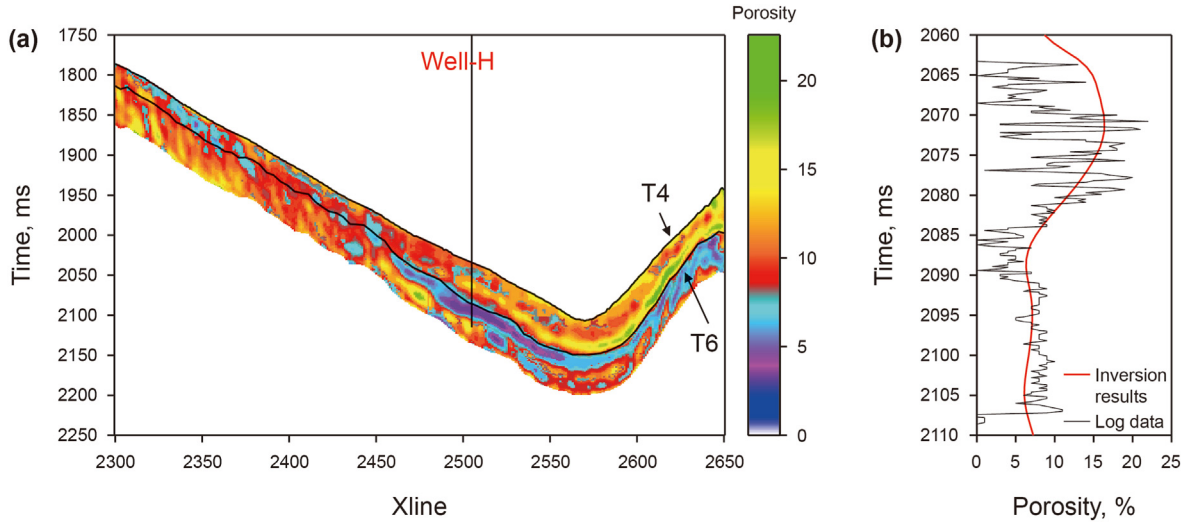

Fig. 13. (a) Porosity prediction results of actual work area (taking the profile of well k119-14 as an example); (b) Comparison results of logging porosity and inversion porosity.

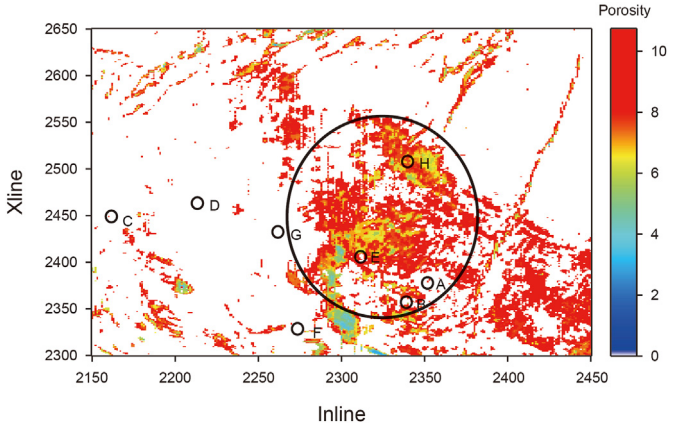

Fig. 14. Porosity prediction results of slices in actual work area (10 ms above layer T6).

the time slice. Therefore, the application of the laboratory-calibrated CPA model provides better inversion results with the help of the velocity dispersion correction, suggesting the important role of accurate frequency-variant rock physics models in the seismic prediction of heavy oil reservoirs.

Declaration of competing interest

I would like to declare that no conflict of interest exists in the submission of this manuscript, and it has approved by all the authors for publication. On behalf of all my co-authors, I assure that the work described was original research that has not been published previously, and not under consideration for publication elsewhere, in whole or in part.

Acknowledgements

This work is supported by NSFC (41930425), Science Foundation of China University of Petroleum, Beijing (No.2462020YXZZ008), R&D Department of China National Petroleum Corporation (Investigations on fundamental experiments and advanced theoretical methods in geophysical prospecting applications (2022DQ0604-01), the Strategic Cooperation Technology Projects of CNPC and CUPB(ZLZX2020-03) and NSFC (42274142).

References

Batzle, M., Hofmann, R., Han, D.H., 2006. Heavy oils— seismic properties. Lead. Edge 25 (6), 750–757. https://doi.org/10.1190/1.2210074.
Behura, J., Batzle, M., Hofmann, R., et al., 2007. Heavy oils: their shear story. Geophysics 72 (5), E175–E183. https://doi.org/10.1190/1.2756600.
Berryman, J.G., 1980. Long-wavelength propagation in composite elasticmedia II. Ellipsoidal inclusions. J. Acoust. Soc. Am. 68 (6), 1820–1831. https://doi.org/10.1121/1.385171.
Ciz, R., Shapiro, S.A., 2007. Generalization of Gassmann's equations for porous media saturated with a solid material. Geophysics 72 (6), A75–A79. https://doi.org/10.1190/1.2772400.
Cole, K.S., Cole, R.H., 1941. Dispersion and absorption in dielectrics, I— alternating current characteristics. J. Chem. Phys. 9, 341–351. https://doi.org/10.1063/1.1750906.
Das, A., Batzle, M., 2008. Modeling studies of heavy oil in between solid and fluid properties. Lead. Edge 27 (9), 1116–1123. https://doi.org/10.1190/1.2978973.
Eastwood, J., 1993. Temperature-dependent propagation of P-waves and S-waves in Cold Lake oil sands: comparison of theory and experiment. Geophysics 58 (6), 863–872. https://doi.org/10.1190/1.1443470.
Gurevich, B., Osypov, K., Ciz, R., et al., 2008. Modeling elastic wave velocities and attenuation in rocks saturated with heavy oil. Geophysics 73 (4), E115–E122. https://doi.org/10.1190/1.2940341.
Han, D.H., Zhao, H.Z., Yao, Q.L., et al., 2007b. Velocity of heavy oil sand. In: 77th Annual International Meeting, SEG, Expanded Abstracts, pp. 1619–1623. https://doi.org/10.1190/1.2792805.
Han, D.H., Liu, J.J., Batzle, M., 2008. Seismic properties of heavy oils —measured data. Lead. Edge 27 (9), 1108–1115. https://doi.org/10.1190/1.2978972.
Han, D.H., Yao, Q.L., Zhao, H.Z., 2007a. Complex properties of heavy oil sand. 77th Annual International Meeting, SEG, Expanded Abstracts 1609–1613. https://doi.org/10.1190/1.2792803.
Makarynska, D., Gurevich, B., Behura, J., et al., 2010. Fluid substitution in rocks saturated with viscoelastic fluids. Geophysics 75 (2), 115–122. https://doi.org/10.1190/1.3360313.
Nur, A., Tosaya, C., Thanh, D.V., 1984. Seismic monitoring of thermal enhanced oil recovery processes. 54th Annual International Meeting, SEG, Expanded Abstracts 118–121. https://doi.org/10.1190/1.1894015.
Russell, B., Dumitrescu, C., Lines, L., 2011. Heavy oil modeling – a tutorial. SEGJ International Symposium 145–150. https://doi.org/10.1190/segj102011-001.36.
Schmitt, D.R., 1999. Seismic attributes for monitoring of a shallow heated heavy oil reservoir: a case study. Geophysics 64 (2), 368–377. https://doi.org/10.1190/1.1444541.
Tosaya, C., Nur, A., Thanh, D.V., et al., 1987. Laboratory seismic methods for remote monitoring of thermal EOR. SPE Reservoir Eval. Eng. 2 (2), 235–242. https://doi.org/10.2118/12744-PA.
Wu, T.T., 1966. The effect of inclusion shape on the elastic moduli of a twophase material. Int. J. Solid Struct. 2 (1), 1–8. https://doi.org/10.1016/0020-7683(66)90002-3.
Xu, S.Y., Payne, M.A., 2009. Modeling elastic properties in carbonate rocks. Lead. Edge 28 (1), 66–74. https://doi.org/10.1190/1.3064148.
Yuan, H.M., Han, D.H., 2013. Pressure and temperature effect on heavy sands properties. SEG Expanded Abstracts 2984–2988. https://doi.org/10.1190/segam2013-1196.1.
Yuan, H.M., Han, D.H., Zhang, W.M., 2016. Heavy oil sands measurement and rock-physics modeling. Geophysics 81 (1), 57–70. https://doi.org/10.1190/geo2014-

0573.1.
Yuan, H.M., Han, D.H., Li, H., et al., 2017. A comparison of bitumen sands and bitumen carbonates: measured data. Geophysics 82 (1), 39–50. https://doi.org/10.1190/geo2015-0657.1.
Yuan, H.M., Han, D.H., Zhao, L.X., et al., 2019. Attenuation analysis of heavy oil sands based on laboratory measurements. Geophysics 84 (5), 299–309. https://doi.org/10.1190/geo2018-0171.1.
Zhao, L.X., Yuan, H.M., Yang, J.K., et al., 2017. Mobility effect on poroelastic seismic signatures in partially saturated rocks with applications in time-lapse monitoring of a heavy oil reservoir. J. Geophys. Res. Solid Earth 122 (11), 8872–8891. https://doi.org/10.1002/2017JB014303.